EXPLICIT VS IMPLICIT NUMERICAL MODELLING OF AIR-COOLED CONDENSER FANS

Adam VENTER[1], Michael OWEN[1],
Jacques MUIYSER[2]

[1] *Stellenbosch University, Department of Mechanical and Mechatronic Engineering, Private Bag X1, Matieland, Stellenbosch 7602, South Africa*

[2] *Howden Netherlands, Haaksbergerstraat 67, Hengelo 7554 PA, Netherlands*

SUMMARY

The implicit fan models used to numerically simulate axial flow fans of air-cooled condensers (ACCs) are only able to provide a limited approximation of actual fan performance within the ACC's complex flow environment. Therefore, to contribute towards deriving new understandings that can facilitate the improvement of these implicit ACC fan models: an explicit fan model formulation, capable of delivering detailed insight into ACC fan behaviour mechanics has been developed here. This model is analysed under low inlet flow rate conditions characteristic of those under which the blade-element based implicit fan models suffer. The presented results highlight the disparity between the implicit and explicit models' determined fan aerodynamic information and provide key insight into important considerations for implicit model improvements.

INTRODUCTION

Air-cooled condensers (ACCs), which find application in Rankine cycle thermoelectric power plants, hold a distinct water-saving and environmental advantage over traditional 'wet-cooled' systems [1]; however, their demand is curtailed by concerns over their susceptibility to losses in efficiency during unfavourable operating conditions. Wind, especially, degrades the cooling capacity of ACCs by exacerbating the flow distortions that occur at the fan unit inlets, re-circulating hot exhaust air and imposing dynamic stresses on the mechanical elements [2]. Accordingly, the study of ACC performance under windy conditions is a popular focus. Regrettably, however, computational fluid dynamic (CFD) analysis of ACC performance under windy conditions is somewhat limited in its ability to accurately simulate ACC behaviour over the full range of likely operating conditions.

By virtue of their scale (for example: the Matimba ACC, South Africa, has 288 10 m diameter fan units [3]), CFD models of ACCs are typically constrained to utilizing some or other implicit

formulation to represent the system's axial flow fans, and it is under windy conditions (low inlet flow rates and separated flow) that the customary implicit formulations are, unfortunately, least reliable [4].

As-of-yet, little information is available on what causes the deterioration of the implicit fan models at both low inlet flow rates [4] and at high cross-flow inlet conditions [5]. Therefore, to contribute towards ultimately bettering numerical ACC wind effect analyses, this study aims to assist in deriving new understandings that can facilitate the improvement of implicit axial flow fan model formulations. To this end, this paper presents a fully explicit three-dimensional (3D) ACC fan model and uses it to gauge the potential shortcomings of the implicit models, guide improvement efforts and advance current understanding of 3D effects in the context of low pressure-rise, low hub-to-tip ratio axial flow fan operation.

NUMERICAL MODELLING OF AXIAL FLOW FANS IN ACCS

Of the axial flow fan modelling methods available to numerical ACC study, implicit pressure-jump and actuator-disk formulations are seemingly the mainstay. The pressure-jump method (PJM), based on the Darcy-Forchheimer approach [6], simulates the operation of an axial flow fan by implementing a discontinuous static pressure jump into the flow field across the fan rotation plane. Whereas actuator-disk methods (ADMs) simulate the operation of an axial flow fan by introducing source terms based on blade-element theory computations, typically referenced on two-dimensional (2D) airfoil lift and drag information [7].

The PJM has been widely utilized in ACC studies, its popularity is attributable to its simple derivation and easy integration into CFD solvers [3]. Due to the nature of its formulation (static pressure rise polynomial function applied over the fan rotation plane), when looking solely at fan static pressure rise prediction, the PJM provides an accurate representation under axisymmetric inflow conditions (for both near design flow rates and low inlet flow rates - conditions under which the pressure rise function is experimentally derived) [4]. However, the performance of the PJM degrades notably in the presence of separated flow features [5]. Consequently, the PJM is not well suited for the modelling of ACC edge fans (peripheral fans in the ACC fan array) where asymmetric separated flow losses predominate [4].

An ADM based on 2D airfoil behaviour accurately predicts fan static pressure rise under axisymmetric inflow conditions at near design flow rates, but its performance degrades markedly at low inlet flow rates (relative to the design point) [8]. At low inlet flow rates, 3D flow effects become distinct [8] and a 3D flow regime is established over the fan blade's sectional profiles; accompanied by (partially understood) complex rotational flow phenomena [9]. The ADM ignores these spanwise flow interactions and the embedded 2D airfoil characteristics become substantially limited [9]. Nonetheless, ADMs are able to provide blade specific information (shaft torque, peak blade bending moment etc.) and offer an improved ACC performance prediction capability for wind effect analyses relative to the PJM; however, only qualitative information is attainable at conditions resembling high wind speeds [5].

To improve the low flow rate performance of the 2D referenced ADM, van der Spuy [4] developed the extended actuator-disk method (EADM). Founded on the insights derived from Himmelskamp [10], the EADM improves low flow fan performance prediction by using augmented lift and drag characteristic information in the source term computation. The EADM accounts for the 3D effects described by Himmelskamp [10] (delayed stall and enhanced lift) by extending the linear character of the two-dimensional lift coefficient through higher angles of attack (with the drag coefficient proportionately modified). However, Himmelskamp [10] only conducted his experiments up to intermediate flow rate conditions (relative to the design point); therefore, van der Spuy [4] had to speculate that stall and reverse flow near the hub (characteristic of low inlet flow rate conditions) would perhaps negate the augmented lift and drag behaviour. The augmented

characteristics are accordingly only provisioned to be utilized above a set radius ratio in the EADM (0.5 recommended for the general case [4]). The EADM, however, still under predicts performance relative to measured values at low inlet flow rates [4].

Blade-element theory based implicit methods also find common application in wind turbine analyses [11] and, likewise, it is recognized that without 3D correction of the airfoil lift and drag polars used in the blade-element consideration, these modelling methods can significantly under predict turbine power outputs [11]. While some effort, like that of van der Spuy [4], has been put towards developing augmentation corrections for the ADMs used in ACC CFD simulations, this effort significantly lags that of the wind turbine industry. The wind turbine industry has invested a particularly large effort into improving their numerical delineation of 3D effects, given its significance to the design and analysis of stall-controlled rotors [13]. Accordingly, multiple correction models have come to fruition over the past decades [14], but their transferability/suitability to ACC axial flow fan models remains unknown. Therefore, this study, in part and in time, also aims contribute towards establishing these parallels.

FULL THREE-DIMENSIONAL, SINGLE FAN CFD MODEL

The fully explicit 3D fan model to be used in investigating the deterioration of the implicit ACC fan models, and to provide insight into 3D effects in the context of low-pressure rise, low hub-to-tip ratio axial flow fans, is presented in this section. The so-called 630 mm eight-bladed L2-fan (scaled operational ACC fan, details of which are available in [15]) with a hub-to-tip ratio of 0.15 has been explicitly defined and incorporated into a model domain representative of the ISO 5801 Type B Standard [16]. The model's solution domain mimics the single fan simulations of Venter *et al.* [5], with the exception that the rotor zone has now been explicitly defined, see Figure 1.

The intent of this study to develop a fully discrete explicit model, instead of the more widespread periodic formulation [9, 15, 17], is conceived in response to the noted uncertainty by Louw [9]. Louw [9], similar to van der Spuy [4], sought to correct the 2D airfoil polynomials used in the traditional ADM by deriving new polynomials fitted to sectional force data determined from his discrete numerical model. The modified polynomials offered improved low flow rate performance prediction under axisymmetric inlet conditions relative to the 2D referenced case, but the ensuing model still underperformed relative to measured data. This underperformance led Louw [9] to question the validity of the periodic boundary conditions used in his discrete model; hence the motivation for a fully explicit assessment here.

Fluid domain and grid generation

The fluid domain and ensuing numerical grid consists of a cubic inlet airspace, a rotor zone encompassing the annular blade passage and fan geometry, and a downstream domain comprising the fan tunnel, see Figure 1. A simplified representation of the fan motor has been included downstream of the fan rotor while the fan shaft, supports and detailed surfaces of the motor have been excluded from the analysis.

The resulting fluid domain was discretized into a conformal polyhedral grid using ANSYS Fluent's meshing capability, see Figure 2. The resulting mesh comprised 18×10^6 cells with a minimal orthogonal quality of 0.15.

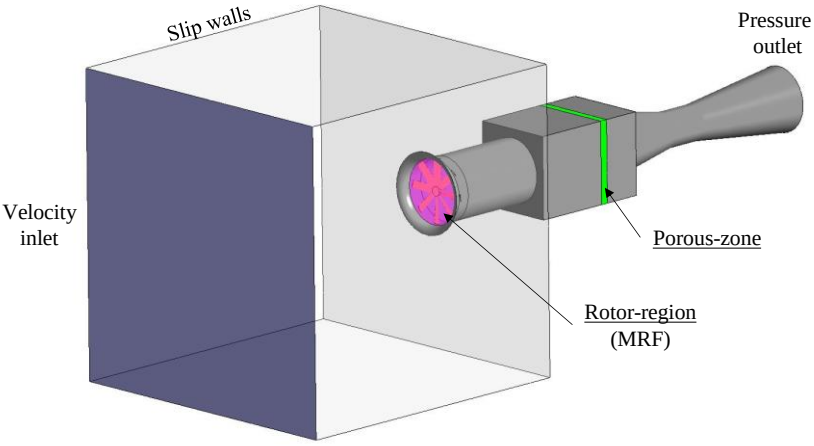

Figure 1: Explicit fan model solution domain

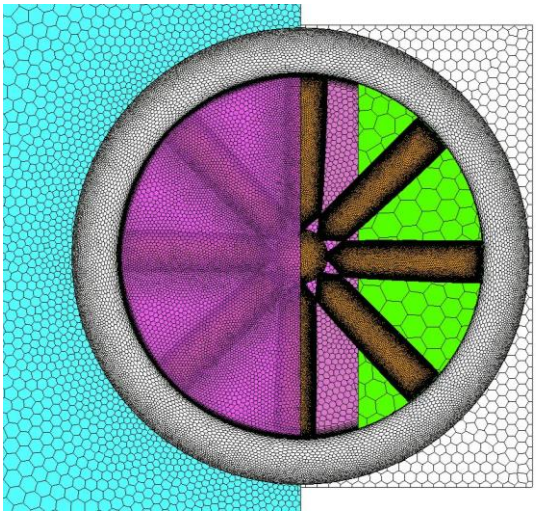

Figure 2: Fluid domain numerical grid

Simulation setup

The double-precision, 3D pressure-based solver available in ANSYS Fluent, version 2021 R2 was used for all the simulations in this study; in conjunction with the SST k-ω turbulence model of Menter [18]. Additionally, the SIMPLE segregated pressure-velocity coupling algorithm and the least-squares gradient calculation method was adopted. The warped face gradient correction functionality available in Fluent was likewise employed, as per its recommended use with polyhedral grids [6].

Following the methodology adopted by Louw [9], a multiple reference frame (MRF) [6] strategy was utilized. A rotational frame motion of 1000 rpm was applied to the rotor region, while the up- and downstream domains remained stationary. Furthermore, a porous-zone formulation was used to represent the hex-core structure present in the downstream plenum chamber of the physical facility, details of which are available in [19].

The solution of each test condition evolved in several steps; initially, a first order up-wind (*UD*) spatial discretization was applied (for all flow variables) and run to convergence. Convergence here was assessed based on a reduction of the flow variable residual values to the order of 10^{-6}, steady pressure monitor values (up- and downstream of the fan rotor region), and the maintenance of mass conservation. From here a linearly blended second-order (*SD*) scheme was adopted for the momentum equation, allowing a greater higher-order term contribution to be applied along with a degree of first-order differencing, which helped to maintain stability. This was achieved through

adjustment of the associated blending factor, Ψ, as shown in Equation (1) [6]. The blending factor was advanced to a value of Ψ = 0.7. The discretization process expresses the value of a scalar quantity ϕ, at a control volume node, p, as a linear combination of the value of ϕ at neighbouring nodes, n:

$$\phi_p = \Psi \sum a_n^{SD} \phi_n^{SD} + (1-\Psi) \sum a_n^{UD} \phi_n^{UD} + S_\phi \quad (1)$$

where a_n are the influence coefficients and S_ϕ is a source term. Stable static pressure rise monitors were observed across the investigated flow range; however, at intermediate flow rates (relative to the design flow rate of 1.45 m^3/s) and below: a slight (~1 %), regular (repetitive) oscillatory behaviour was observed in monitored blade force values. A time-dependent assessment is, therefore, seemingly required to obtain converged second-order accuracy for these conditions; however, a transient analysis is beyond the scope of this paper (transient analyses are being considered as part of a broader study). Rather, histories of the oscillatory solutions were sampled to capture representative averages. Averaged pressure, wall shear stress and velocity values were subsequently used in all processed data. All simulations were performed using the Centre for High Performance Computing's (CHPC's) Lengau cluster, providing 240 parallel processors for each run.

RESULTS

The determined fan static pressure rise and shaft power results from the 3D explicit model are presented in Figure 3. Included in Figure 3a is the ADM (2D airfoil data formulation) and EADM results from Venter [19]; the results in Figure 3 are compared to their experimental counterparts as determined by Marincowitz *et al.* [20].

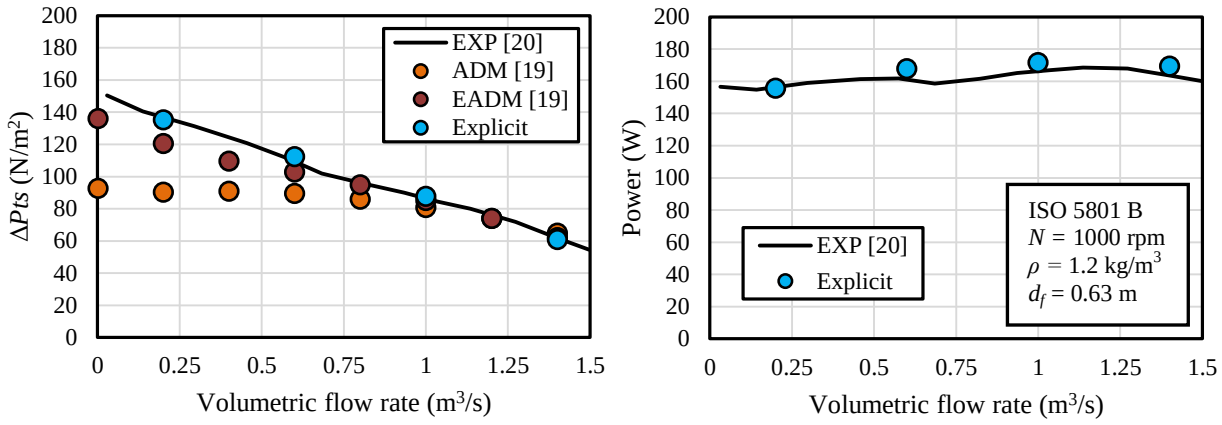

Figure 3: Fan characteristic results
(a) Fan static pressure rise (b) Fan shaft power

With reference to Figure 3a and 3b: a close correspondence to measured data is attained with the explicit model across the full investigated flow range. Conversely, in Figure 3a, it is seen that both the ADM and EADM's performance starts to deviate from measured values near a flow rate of $\dot{V}$ = 1 m³/s.

To gain insight into potential causes for the implicit models' falling performance, comparative aerodynamic information is generated. To attain this aerodynamic information, blade sectional force (pressure and wall-shear) and free-stream velocity information has been extracted at multiple span-wise locations from a single representative blade of the explicit model (see Figure 4) at various flow rates.

Two different free-stream velocity evaluation methods have been utilized here. Using two different velocity evaluation methods provides the opportunity to gauge the potential effect the velocity calculation has on the description of 3D effects and the implicit models' performance. The first method (V1) is consistent with the ADM/EADM formulation: the resultant free-stream velocity is determined by averaging axial and tangential velocity information taken at a distance approximately 0.5 chord lengths up- and downstream of each radial blade section. For the second method (V2), velocity information at each radial section is determined by averaging the axial and tangential velocity data found along the surrounding contours. The velocity surfaces in this case were set to extend from its corresponding blade contour at an iso-distance of $0.15 \times r$, where r is the radial position. The iso-surfaces scale along the blade to account for the increasing solidity, and to maintain an isolated airfoil assessment.

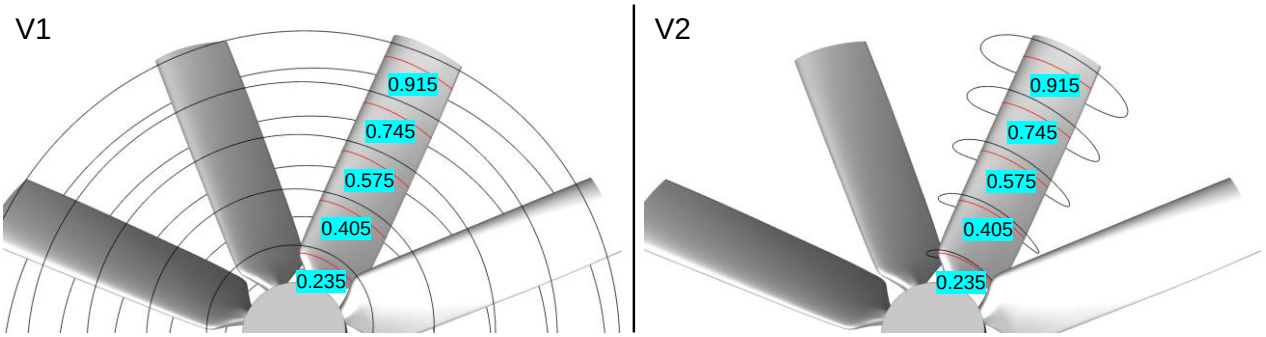

Figure 4: Fan blade data iso-surfaces

Figure 5 shows the determined spanwise aerodynamic information at $\dot{V}$ = 1, 0.6 and 0.2 m³/s, calculated using the V1 velocity evaluation method. The top row of graphs corresponds to the flow condition of $\dot{V}$ = 1 m³/s, while the middle and bottom rows correspond to $\dot{V}$ = 0.6 and 0.2 m³/s respectively. The 1st column captures the spanwise angle of attack and relative velocity magnitude extracted from the explicit model for each flow rate. The 2nd and 3rd columns detail the corresponding lift and drag information at the given spanwise positions. Included in Figure 5 is the equivalent 2D lift and drag characteristics as well as the augmented characteristics that would be utilized in the EADM source term computation for the given angles of attack. This comparative implicit model information has been determined by passing the spanwise angles of attack into the respective lift and drag polynomial expressions used by the ADM and EADM models of Venter [18].

Figure 6 shows the same, but for the information determined using the V2 velocity evaluation method. The V2 velocity evaluation method uncovers exceptionally large coefficient values in the near root region of the fan blade (which is expectedly due to the high blade solidity in this region). The depicted lift and drag coefficient ranges of the graphs in Figure 6 have, however, been restricted to provide sufficient clarity to the majority of the spanwise data points and excludes details of the explicit data points at the lowest investigated radius ratio (*RR*). Information on these omitted data points can accordingly be found in Table 1.

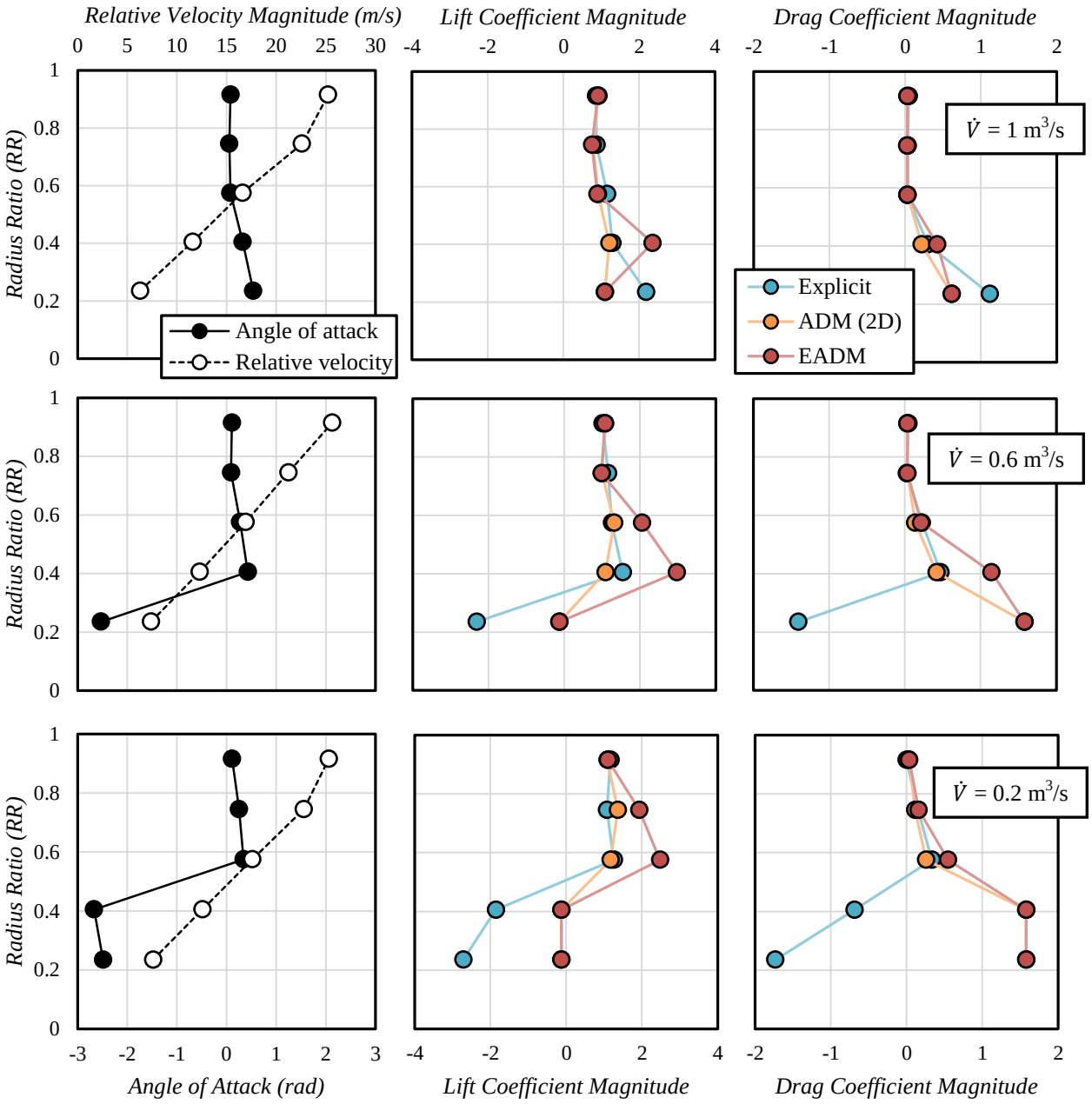

Figure 5: Comparative aerodynamic information, determined via the V1 velocity evaluation method (top row) $\dot{V}$ = 1 m^3/s (middle row) $\dot{V}$ = 0.6 m^3/s (bottom row) $\dot{V}$ = 0.2 m^3/s

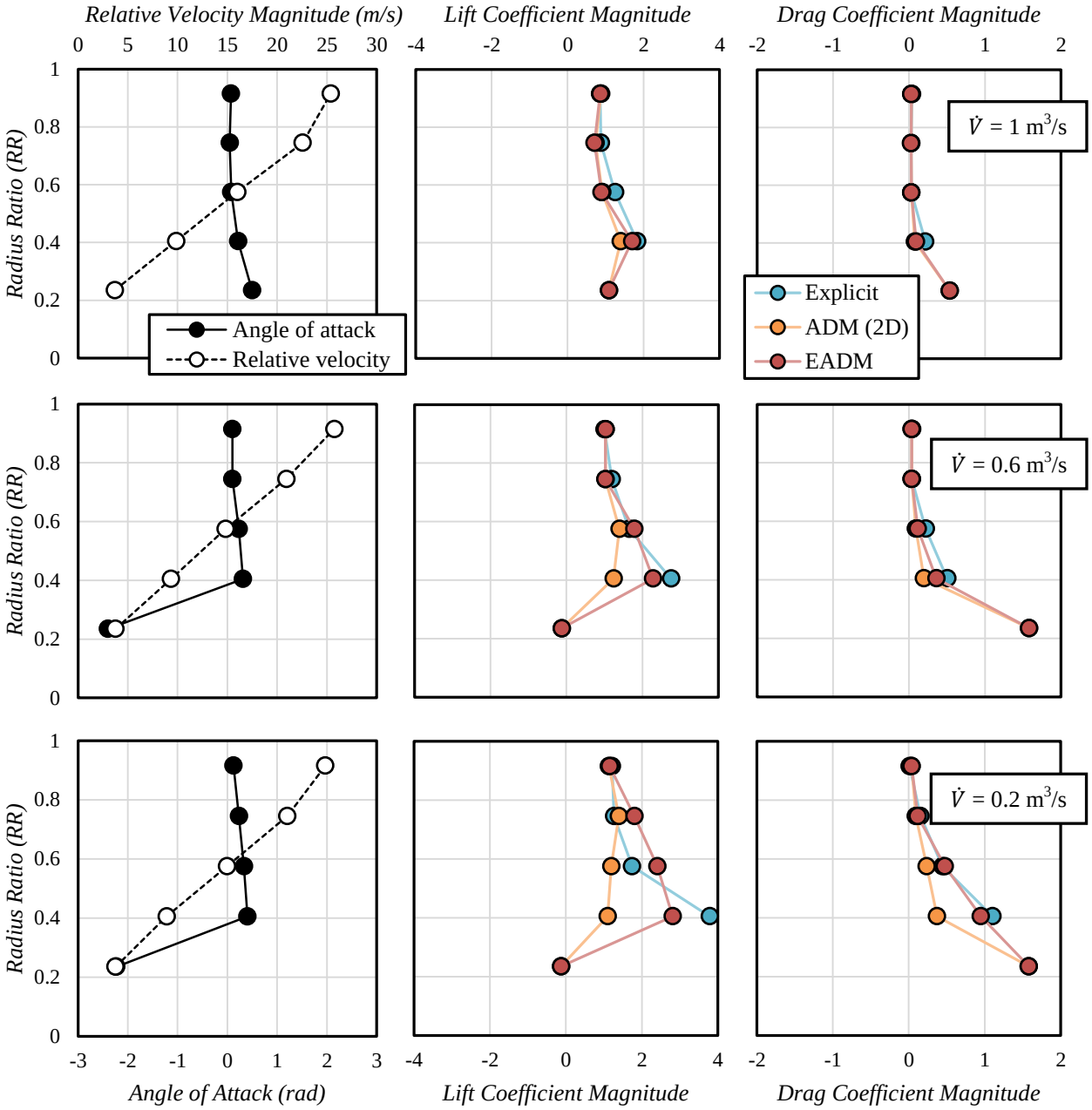

Figure 6: Comparative aerodynamic information, determined via the V2 velocity evaluation method (top row) $\dot{V}$ = 1 m³/s (middle row) $\dot{V}$ = 0.6 m³/s (bottom row) $\dot{V}$ = 0.2 m³/s

Table 1: Explicit model data points at RR = 0.235 not depicted in the graphs of Figure 6

$\dot{V}$ (m³/s)	Lift Coefficient Magnitude	Drag Coefficient Magnitude
1	6.45	2.95
0.6	-8.14	-6.53
0.2	-9.03	-9.69

Considering Figure 5: expectedly, a noticeable deviation between the lift and drag data sets is observed as the flow rate reduces. At $\dot{V} = 1$ m³/s, the explicit 3D (rotational) and static 2D aerodynamic response is comparable over the bulk of the outer blade span; only significantly departing from one another near the root of the blade (hence the comparable results in Figure 3 at this flowrate). At this flowrate, 3D effects seem to be concentrated to the near root region (as evidenced by the notable difference between the 3D and 2D data in this region), which contrasts with the EADM formulation as no augmentation is applied until a $RR = 0.4$ in this case [18]. At the lower flowrates, the presence of reverse flow is noted by the negative angles of attack, and here the static 2D and augmented EADM aerodynamic characteristics bear little resemblance to the explicit 3D case. Based on this data determined via the V1 evaluation method, it is apparent that the EADM augmentation fails to correctly handle the presence of reverse flow and seems to falsely inflate the lift coefficient in the outer blade span. This suggests that 3D effects are ill described by the implemented augmentation of the EADM.

Interestingly, however, when considering Figure 6: a different verdict is evidently apparent. When assessing the data determined via the V2 evaluation method, the augmentation of the EADM appears to be considerably better at capturing the 3D effects than it did in Figure 5. Again, the greatest distinction between the data sets is observed in the near root region, where no augmentation is implemented by the EADM (however, the explicit model data is allegedly exacerbated by the high blade solidity in this region).

Another interesting facet emerges from the results of Figure 6: at $\dot{V} = 0.6$ m³/s (at the spanwise positions where augmentation is actioned) the EADM's augmented character closely mimics the 3D results; however, at $\dot{V} = 0.2$ m³/s, the EADM's augmentation overly exaggerates the lift enhancement. This (together with the notes of the preceding paragraphs) suggests that potential improvements to the EADM lie in the revised treatment of 3D effects in the near root region and through the scaling of the implemented augmentation with flowrate. It is, however, cautioned that the strong 'near-hub' effect present in this case may just be an artefact of the investigated fan's design and low hub-to-tip ratio, and that these results are perhaps not representative of the general axial flow fan case. Further investigation, across multiple fan types is therefore motivated.

Critically important to note is the distinct effect the velocity evaluation method is shown to have on the description of the aerodynamic information. Between Figures 5 and 6, the effectiveness of the EADMs' augmentation and the differences between the static 2D and 3D information are starkly dissimilar. Accordingly, for the development of future implicit methods, it is clear that the specification of the aerodynamic augmentation must be appropriately described relative to the velocity determination method for the given model. Furthermore, the results show the velocity determination warrants careful consideration given the observed sensitivity of the information.

CONCLUSION

A full 3D explicit fan model of a low-pressure rise, low hub-to-tip ratio ACC fan has been successfully simulated under ideal inlet flow conditions. The model has been demonstrated to be a promising tool for use in gaining insight into the reasons commonly used implicit ACC axial flow fan models deteriorate at low inlet flow rates. For the investigated fan: the lift and drag characteristics determined from the explicit model were shown to differ considerably from that of their 2D counterparts and the augmented characteristics of the EADM fan model. It is observed that the considered actuator-disk formulation models could seemingly benefit from a revised treatment of 3D effects at near root blade sections and from the scaling of implemented augmentations with flowrate. Furthermore, the sensitivity of implicit actuator-disk formulations to the free-stream velocity consideration was also demonstrated. The results of this study assist in delivering new insight that can be used to develop and ultimately contribute towards the improved simulation of ACC axial flow fans using low-cost implicit models and thus also the progression of ACC wind effect research.

BIBLIOGRAPHY

[1] EPRI. *Economic Evaluation of Alternative Cooling Technologies*, Palo Alto, CA: 1024805, **2012**

[2] Maulbetsch, J. and DiFilippo, M. – *The Use of Wind Barriers To Mitigate the Effect of Wind on Air-Cooled Condensers*, California Energy Commission. Publication number: CEC-500-2016-047, **2016**

[3] Fourie, N., van der Spuy, S.J. and von Backström, T.W. – *Simulating the Effect of Wind on the Performance of Axial Flow Fans in Air-Cooled Steam Condenser Systems*, Journal of Thermal Science and Engineering Applications, 7(2), pp. 021011-021012, **2015**

[4] van der Spuy, S.J. – *Perimeter Fan Performance in Forced Draught Air-cooled Steam Condensers*. PhD Dissertation, Department of Mechanical and Megatronic Engineering, University of Stellenbosch, **2011**

[5] Venter, A.J., Owen, M.T.F. and Muiyser, J. – *Numerical analysis of windscreen effects on air-cooled condenser fan performance and blade loading*, Applied Thermal Engineering, 186, pp. 1-11, **2020**

[6] Fluent. *ANSYS Fluent documentation*, ANSYS Inc, **2009**

[7] Thiart, G.D. and von Backström, T.W. – *Numerical simulation of the flow field near an axial flow fan operating under distorted inflow conditions*, Journal of Wind Engineering and Industrial Aerodynamics, 45, pp. 189-214, **1993**

[8] Meyer, C.J. and Kröger, D.G. – *Numerical simulation of the flow field in the vicinity of an axial flow fan*, International Journal for Numerical Methods in Fluids, 36, pp. 947-969, **2001**

[9] Louw, F.G. – *Investigation of the flow field in the vicinity of an axial flow fan during low flow rates*. PhD Dissertation, Department of Mechanical Engineering, University of Stellenbosch, **2015**

[10] Himmelskamp, H. – *Profile investigations on a rotating airscrew*. PhD Dissertation, University of Göttingen, **1945**

[11] Dumitrescu, H., Frunzulica, F. and Cardos, V. – *Improved Stall-Delay Model for Horizontal-Axis Wind Turbines*, Journal of Aircraft, 50(1), pp. 315-319, **2013**

[12] Guntur, S. – *A Detailed Study of the Rotational Augmentation and Dynamic Stall Phenomena for Wind Turbines*. PhD Dissertation, Wind Energy Department, Technical University of Denmark, **2013**

[13] Gur, O. and Rosen, A. – *Propeller Performance at Low Advance Ratio*, Journal of Aircraft, 42(2), pp 435-441, **2005**

[14] Brenton, S.P., Coton, F.N. and Moe, G. – *A Study on Rotational Effects and Different Stall Delay Models Using a Prescribed Wake Vortex Scheme and NREL Phase VI Experiment Data*, Wind Energy, 11, pp. 459-482, **2008**

[15] Augustyn, P.H. – *Experimental and Numerical Analysis of Axial Flow Fans*. MscEng Thesis, Department of Mechanical Engineering, University of Stellenbosch, **2013**

[16] Herraez, I., Stoevesandt, B. and Peinke, J. – *Insight into Rotational Effects on a Wind Turbine Blade Using Navier-Stokes Computations*, Energies, 7, pp. 6798-6822, **2014**

[17] ISO 5801 – *Industrial fans: Performance testing standardized airways*, international organization for standardization **2007**

[18] Menter, F.R. – *Two-equation eddy-viscosity turbulence models for engineering applications*, AIAA Journal, 32(8), pp. 1598-1605, **1994**

[19] Venter, A.J. – *Numerical analysis of windscreen effects on air-cooled condenser fan performance and blade loading*. MScEng Thesis, Department of Mechanical Engineering, University of Stellenbosch, **2020**

[20] Marincowitz, F.S., Owen, M.T.F. and Muiyser, J. – *Experimental investigation of the effect of perimeter windscreens on air-cooled condenser fan performance*, Applied Thermal Engineering, 163, pp. 1-9, **2019**